V_2O_5 Graphene Hybrid Supported on Paper Current Collectors for Flexible Ultra-High-Capacity Electrodes for Lithium-Ion Batteries

Nojan Aliahmad [1,2,4], Yadong Liu [3,4], Jian Xie [3,4*], and Mangilal Agarwal [3,4*]

[1] Department of Electrical & Computer Engineering, Indiana University-Purdue University Indianapolis (IUPUI), Indianapolis, IN, 46202, USA

[2] School of Electrical & Computer Engineering, Purdue University, West Lafayette, 47907, USA

[3] Department of Mechanical Engineering, Indiana University-Purdue University Indianapolis (IUPUI), Indianapolis, IN, 46202, USA

[4] Integrated Nanosystems Development Institute (INDI), Indiana University-Purdue University Indianapolis (IUPUI), Indianapolis, IN, 46202, USA

Corresponding authors: agarwal@iupui.edu, jianxie@iupui.edu

This is the author's manuscript of the article published in final edited form as:

Aliahmad, N., Liu, Y., Xie, J., & Agarwal, M. (2018). V2O5 Graphene Hybrid Supported on Paper Current Collectors for Flexible Ultra-High-Capacity Electrodes for Lithium-Ion Batteries. ACS Applied Materials & Interfaces. https://doi.org/10.1021/acsami.8b02721

Abstract

An ultra-high capacity, flexible, electrode made with a vanadium pentoxide/graphene (with the specific capacity of 396 mAh/g) supported on paper-based current collectors has been developed. The ultra-high capacity graphene-modified vanadium pentoxide is fabricated by incorporating graphene sheets (2 wt.%) into the vanadium pentoxide nanorods to improve the specific capacity, cycle life and rate capability. This active material is then incorporated with the paper-based collectors (CNT-microfiber paper currents), to provide flexible electrodes. The flexible current collector has been made by depositing single-wall carbon nanotubes (CNT) over wood microfibers through a layer-by-layer (LbL) self-assembly process. The CNT mass loading of the fabricated current collectors is limited to 10.1 μg/cm^2. The developed electrodes can be used to construct the flexible battery cells, providing a high capacity/energy and rechargeable energy storage unit for flexible electronic devices.

Keywords: Flexible batteries, Paper-based batteries, Ultra-high capacity, flexible current collector, V_2O_5/graphene, carbon nanotube, lithium ion

Introduction

Recent advancements in flexible electronics have resulted in the strong demand for flexible power sources with high specific capacity/energy. Lithium-ion batteries (LIBs) can effectively provide the energy and power needed for flexible electronics such as wearable devices, flexible displays, and printable electronics with high specific capacity/energy, rechargeability, and durability. Efforts have been dedicated to make flexible lithium-ion batteries using conventional electrode materials with little progress because of the failure from repeated bending [1-3]. Flexible electrodes are the key for making flexible batteries and require a flexible current collector capable of integrating the active electrode materials to form a cohesive, durable, highly conductive, robust, and bendable electrode. Despite all the progress on making flexible lithium ion batteries, achieving a fully bendable/flexible and highly conductive electrode with high specific capacity/energy remains a huge challenge. Depositing conductive carbons over plastic substrates or papers is an effective approach for making flexible current collectors. Carbon nanotubes (CNTs) can act as the conductive carbon in flexible current collectors due to their high conductivity and mechanical stability [4-7]. These paper like current collectors can provide flexibility, are lightweight, and have a high capacity for lithium-ion batteries due to their high porosity and stability. A conductive sheet can be made by applying CNT inks over a paper or directly depositing CNTs into a paper and forming a bulky paper. While CNT-coated paper can provide a flexible current collector, the fabrication cost is quite high due to the large amount of CNTs used. Furthermore, these methods cannot preserve all the properties of paper such as its high porosity.

Presented here is a novel method of making flexible and highly conductive electrodes consisting of (i) fabricating paper-based current collectors with CNT usage at less than 10 $\mu g/cm^2$ and (ii) making a high specific capacity/energy electrode using such a current collector. In this method, the wood microfibers are coated with layers of CNTs using a layer-by-layer (LbL) self-assembly method and then are transformed into a single CNT-microfiber paper sheet. While this CNT-microfiber paper provides excellent flexibility and conductivity, it can simultaneously be used as the current collector. The CNT usage to make this CNT-microfiber paper is 10 times lower than other reported CNT-based current collectors [8]. While quite large amount of CNT is used to make bulky papers in the fabrications of other CNT-based current collectors, in our method, the CNT usage is only 0.2 wt.% of the fabricated paper. In addition, this method preserves the properties of the paper such as its high porosity and mechanical stability. Furthermore, the LbL method can preserve the properties of the paper microfibers such as porosity, flexibility and high absorption. The LbL assembly can be integrated in paper-making process to reduce the complexity of making these CNT papers. This method can provide fully flexible current collectors while reducing the fabrication cost.

In conjunction with the CNT-microfiber paper, having a high capacity cathode material is also a challenge of making flexible lithium-ion batteries. Different metal oxides such as $LiNi_{1/3}Mn_{1/3}Co_{1/3}O_2$ (160 mAh/g) [9], $LiFePO_4$ (170 mAh/g) [10], and $LiMn_2O_4$ (120 mAh/g) [11] have been developed [12-13]. These materials can provide sufficient capacity and cycle life, although their theoretical specific capacity is still not high enough for the next generation of lithium-ion batteries in applications such as electric cars or portable electronics. To achieve higher specific capacity/energy, novel materials are needed. In this case, vanadium oxides are good candidates for high specific capacity/energy due to their multi-valence change during the charge/discharge process. Vanadium pentoxide (V_2O_5) has a theoretical capacity of 443 mAh/g (assuming intercalation of three-lithium ions) and a specific energy of 1218 Wh/kg (assuming a nominal 2.75 V discharge voltage). The challenges for realizing a high specific capacity/energy in practical LIB applications [14-20] lies in these three issues: (1) low electron conduction, (2) slow lithium-ion diffusion, and (3) irreversible phase transitions upon deep discharge. Recently, we have developed a nanostructured hybrid V_2O_5 material in which a small amount of graphene (1-2 wt.%) is incorporated between V_2O_5 nanoribbons [21]. Such a nanostructured V_2O_5/graphene (V_2O_5/G) hybrid effectively solved the three issues mentioned above by (1) providing the intra-particle and inter-particle electronic conductivity for V_2O_5 nanoribbons, (2) improving the Li^+ ion diffusion to form smaller ribbons, and (3) keeping the structure integrity because the graphene sheets hold the V_2O_5 nanoribbons. Such a nanostructured hybrid V_2O_5/G material exhibits the excellent cyclability and rate performance while achieving theoretical capacity. In this work, this novel nanostructured V_2O_5/G hybrid is used to make flexible electrodes with paper current collectors.

Experimental

Paper-Based Current Collectors

The CNT-microfiber current collectors were fabricated from bleached Kraft softwood microfibers (less than 1% lignin and 99% cellulose). These fibers were individually coated with layers of CNT through a layer-by-layer (LbL) nano-assembly. An aqueous dispersion of poly(3,4-ethylenedioxythiophene)-poly(styrenesulfonate) (PEDOT-PSS) (Heraeus Clevios) conductive polymer (3 mg ml^{-1}) and carbon nanotubes (NanoIntegris Inc.) (25 μg ml^{-1}) were used as the anionic conductive materials. The cationic component was the aqueous solution of poly-(ethyleneimine) (PEI) (3 mg ml^{-1}). The wood microfibers were coated with four bi-layers of PEI/CNT in alternate with two bi-layer of PEI/PEDOT-PSS. To deposit the layer through LbL process, the fibers are soaked in the described aqueous solutions, for 10 minutes and then washed with Mili-Q water. Figure 1 shows the LbL process and the deposition of every layer over the fibers following by rinsing with Mili-Q water to remove the residues from the previous steps. The thicknesses of the deposited layers made with LbL method have been estimated using the

assembled films of the multilayers over a silver electrode resonator of a quartz crystal microbalance (QCM,9 MHz, USI-System, Japan).

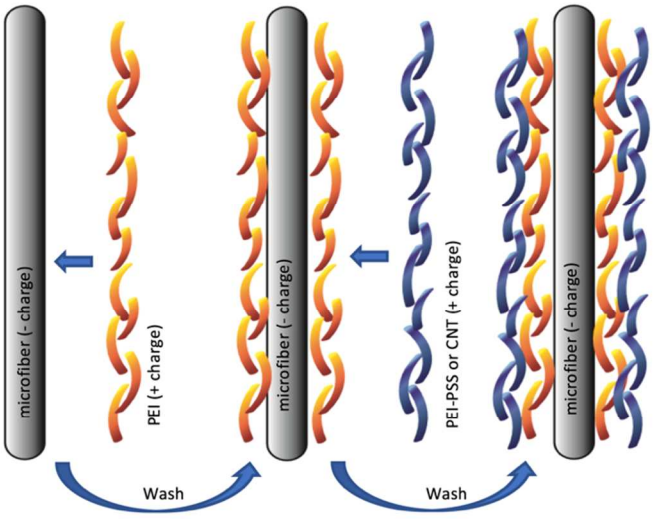

Figure 1. Schematic of the LbL process of depositing oppositely charged polyelectrolytes to coat paper microfibers

In the next step, the coated microfibers were assembled into a paper sheets using a homemade setup (meeting the standard of Technical Association of Pulp and Paper (TAAPI) T 205T) and then dried in vacuum oven to be used as the current collector. In this technique, the properties of the paper such as porosity and texture were preserved while a coating of CNT provided electric conductivity to the paper sheets. In addition, applying the LbL technique limited the CNT usage to only 0.2 wt.%. The conductivity of the fabricated CNT-microfiber paper was measured using Keithley 4200 IV (Tektronix USA) and the structure of that was examined using Bruker D8 Discover X-Ray Diffraction (XRD) (Bruker USA).

Electrode Fabrication, Cell Assembly and Characterization

V_2O_5/G was synthesized by the novel and simple method of incorporating graphene sheets into the nanostructure of V_2O_5 xerogel via a sol–gel process and forming a graphene-modified V_2O_5 hybrid with a stabilized layered structure [21]. The V_2O_5/G, Super P Li (TIMCAL), and PVDF (Kynar) were mixed and dissolved in N-Methyl-2-pyrrolidone (NMP) with a ratio of 85:10:5 by weight. The loading of the active material (V_2O_5/G) is around 0.4 mg/cm^2. This solution then was sprayed over the CNT-microfiber paper to make electrodes. The fabricated electrodes were dried overnight in a vacuum oven and then transferred to the argon-filled glovebox. The pouch cells (electrode dimension: 3 cm x 5 cm, cell capacity: 2.4 mAh) and coin cells (electrode geometric area: 2 cm^2, cell capacity: 0.8 mAh) were made using lithium foil and V_2O_5/G electrodes and Celgard 2400 separators. 90 µL liquid electrolyte was then added to the battery assembly, a 1.0 M lithium phosphorous fluoride ($LiPF_6$) in an ethylene carbonate/diethyl carbonate

(EC/DEC) mixture (1:1 by volume). After assembly, cells were left overnight to reach to their stable state before testing. The fabricated devices were tested using an Arbin BT2000 battery testing system. All the chemicals for the experiments have been supplied by Sigma-Aldrich unless the vendor is noted. The formation of the electrolyte layer over the CNT-microfiber paper current collectors, and the damages/deformations of the electrolyte layer after bending test were analyzed by JEOL 7800F Field Emission Scanning Electron Microscope (FESEM) (JEOL Japan) images.

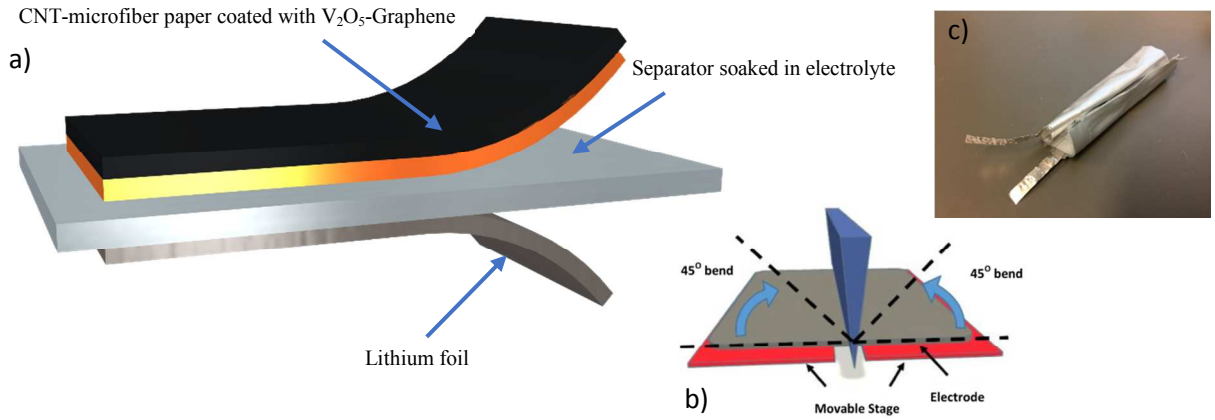

Figure 2. a) Schematics of the paper-based V_2O_5 cell, b) the bending test set-up, and c) a completely bended paper-based pouch cell

Cyclic Voltammogram (CV) Test

In order to investigate the electrochemical stability of the CNT paper, CV experiments were carried out. Two types of V_2O_5/G electrodes (Al foil and CNT paper) were used as the working electrodes. Li metal served as both counter electrode and the reference electrode (figure 2). The potential window for cyclic voltammetry was set from 1.5 V to 4.0 V (vs. Li/Li^+) as the typical voltage range for a cathode, with a scan rate of 5.0 mV/s using a 1470E Multistat (Solartron Analytic, UK). Another CV experiment was carried out from 0.0 V to 4.0 V (vs. Li/Li^+) with a scan rate of 5.0 mV/s to evaluate the electrochemical stability of the current collector in harsh conditions.

Electrochemical Impedance Spectroscopy (EIS) Characterization

EIS was employed to characterize the internal impedance changes of V_2O_5/G cells with an Al foil current collector and a CNT paper current collector, respectively. A Solartron 1287A/1260A Potentiostat/Impedance System (Solartron Analytical, England, UK) was used to measure the AC impedance of these cells in the frequency range of 0.01 Hz–1 MHz with a voltage amplitude of 5.0 mV.

Results and Discussion

Paper-Based Electrodes

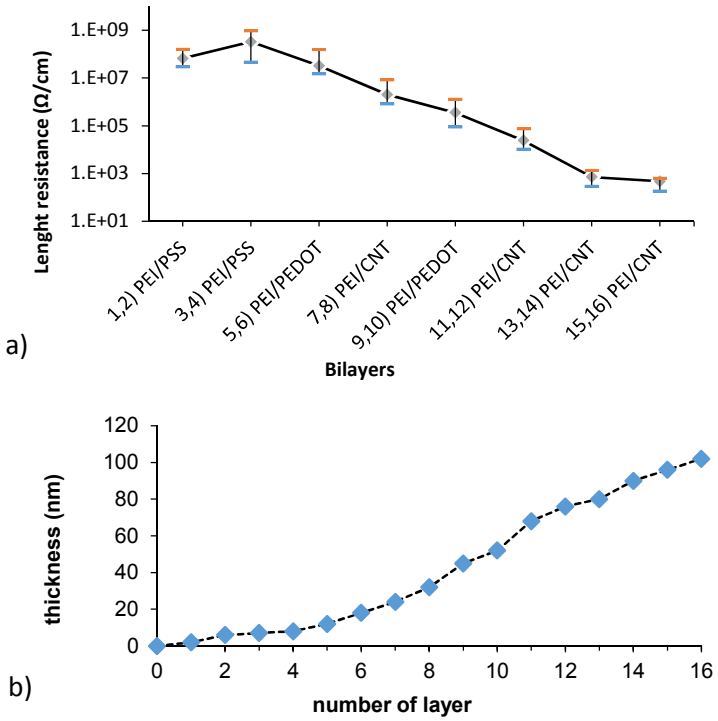

Order of the deposited layers over paper fibers	
Layers	**Material**
1	PEI
2	PSS
3	PEI
4	PSS
5	PEI
6	PEDOT:PSS
7	PEI
8	CNT
9	PEI
10	PEDOT:PSS
11	PEI
12	CNT
13	PEI
14	CNT
15	PEI
16	CNT

Figure 3. (a) Length resistance of the wood microfibers after deposition of each bi-layer of PEDOT or CNT. The error bars indicate the minimum and maximum of the measured resistivity with the data points showing the mean values, and (b) thickness of each coated layer over the wood microfibers.

To check the formation of conductive layers over the paper microfibers through the LbL process, the resistivity of the microfibers was measured after adding each bi-layer. The resistance of each fiber and dimension of each fiber was measured using a Keithley CV measurement with a microprobe station. Figure 3a shows the average, minimum, and maximum length resistance (resistance/ length of the microfibers) of 20 microfibers chosen randomly after adding each bilayer. The results show that by adding the bi-layers of PEI/PEDOT-PSS or PEI/CNT, the resistance of the microfibers decreases. These layers with the thickness of 5 nm, form a conductive layer around the fibers and reduce the resistivity of the microfibers exponentially. The Figure 3b shows the thickness of different LbL layers over the fibers, measured by QCM. The measured the total thickness of the deposited LbL layers over the fibers is in the range of 100 nm. While the diameter of the wood microfibers is in the range of 35-50 µm, the thickness of the coated layer is counted 2 to 3% of the total thickness of the CNT coated microfibers [8]. The electrical pathway over the microfibers has been made by continued conductive networks of CNT rods over a layer of PEDOT-PSS. It was previously reported that this conductive pathway improves the conductivity of the CNT-microfibers, while the CNT layers on top of the PEDOT-PSS layer limit the conductivity fade of the PEDOT-PSS. The length resistance of CNT-microfiber after adding 8 bilayers of

PEI/CNT was measured to be 0.468 kΩ/cm. The resistance degradation of the CNT-microfiber is less than 10% within 6 months after fabrication [6, 8]. In addition, the CNT mass loading of the fabricated paper-based current collectors is about 10.1 μg/cm^2 and the PEDOT:PSS mass loading in such a current collector is 100 μg/cm^2. The XRD of the CNT-microfiber paper is demonstrated in Figure 4. Comparing the CNT-microfiber paper (made by using the CNT solution) with the CNTs, it is clear that the CNTs are attached to the surface of the microfiber. The peak at 24º is related to the anisotropy of the 002 plane of the CNTs. This strong peak is visible in both CNT-microfiber paper and the CNT:PSS sample, indicating the attachment of the CNT:PSS layer over the paper microfibers [22].

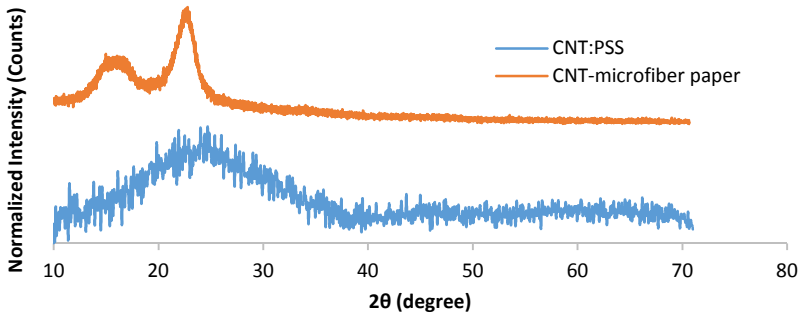

Figure 4. XRD pattern of the CNT-microfiber paper and CNT layer over the glass substrate. Here the base lines of the samples are different, and the intensity has been normalized

The paper electrodes and metallic current collectors, respectively, were tested through different bending tests. Both the CNT-microfiber paper and aluminum foil were coated with a V_2O_5/G layer, respectively and then bent to 90º for 20 times. The bending test is shown in the inset of Figure 2. Here the electrode was fixed to two bendable stages and bent to a 90º angle. The fractures and deformations of the electrode were examined using FESEM. For comparison, conventional electrodes of the V_2O_5/G layer using the metallic current collectors (spraying the same V_2O_5/G materials over the aluminum foil) were also prepared. These conventional electrodes were also tested for bendability under the same conditions. The morphologies of both electrodes were examined using FESEM and energy dissipative spectroscopy (EDS) before and after the bending test to observe the fractures and the damages to the electrodes after bending test, shown in Figure 5 (top view) and Figure 6 (cross-section). The EDS results also revealed the sulfur for coated CNT-microfiber paper, aluminum for metallic current collectors and vanadium for V_2O_5 active material layer over the electrodes. As can be seen, for the conventional electrode, some V_2O_5/G layers were completely detached from the location of the fracture of the metal current collector, while the V_2O_5/G layer was intact over the paper-based current collector. Additionally, some V_2O_5/G layers were seen starting the detachment from the surface of the metal current collector. It is anticipated that the air gaps and cracks in the conventional electrode after bending will result in a lower cycle life and reduced

capacity and rate performance due to the increased internal resistance of the electrodes up to 300%. On the other hand, the paper-based electrodes are almost intact after bending, while only small portions over the fracture show some tiny cracks without significant detachment of the V_2O_5/G layer from the paper based current collector. The internal resistance change of the paper-based electrodes after bending was observed to be only 50%. Such good electrode integrity may be attributed to the porous structure of the paper current collector that leads to the increased adhesion between the V_2O_5/G layer and the paper current collector. In addition, the V_2O_5/G particles entangle with the fabrics of the paper current collector to form an integrated layer with strong bonding between the layers, which, in turn, leads to improved stability and performance of the electrode as well as improved flexibility.

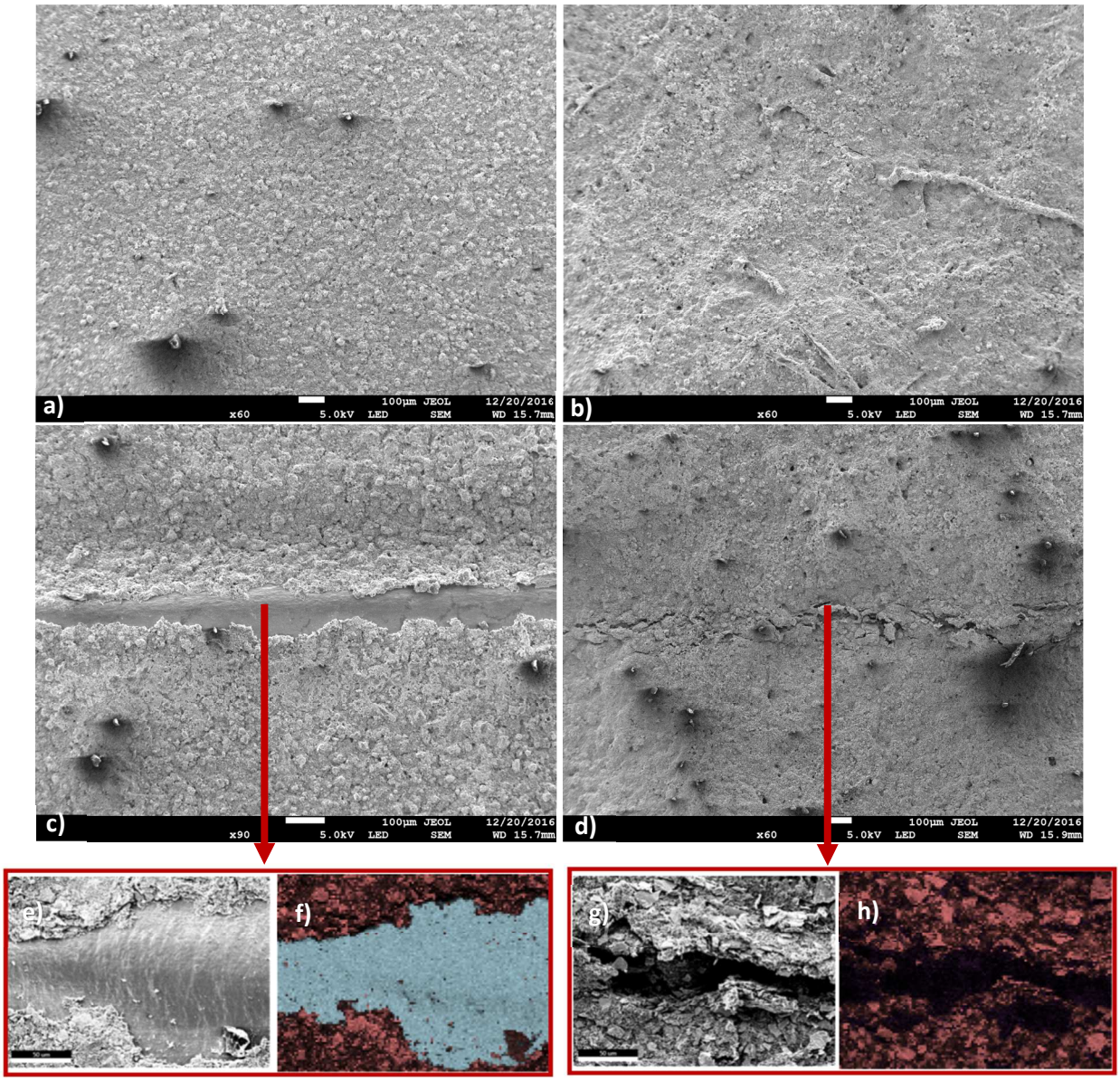

Figure 5. FESEM images of a) metallic and b) paper-based electrodes before bending test, and c) metallic and d) paper-based electrodes, all electrodes were bend 90º for 20 times (the insets of the images are showing the existence of aluminum for metallic cells, sulfur for CNT-microfiber paper and vanadium using the energy dissipative spectroscopy after the bending test), e) SEM, and f) EDS of the crack formation over metallic electrodes, g) SEM and h) EDS of the crack formation over the paper-based electrodes

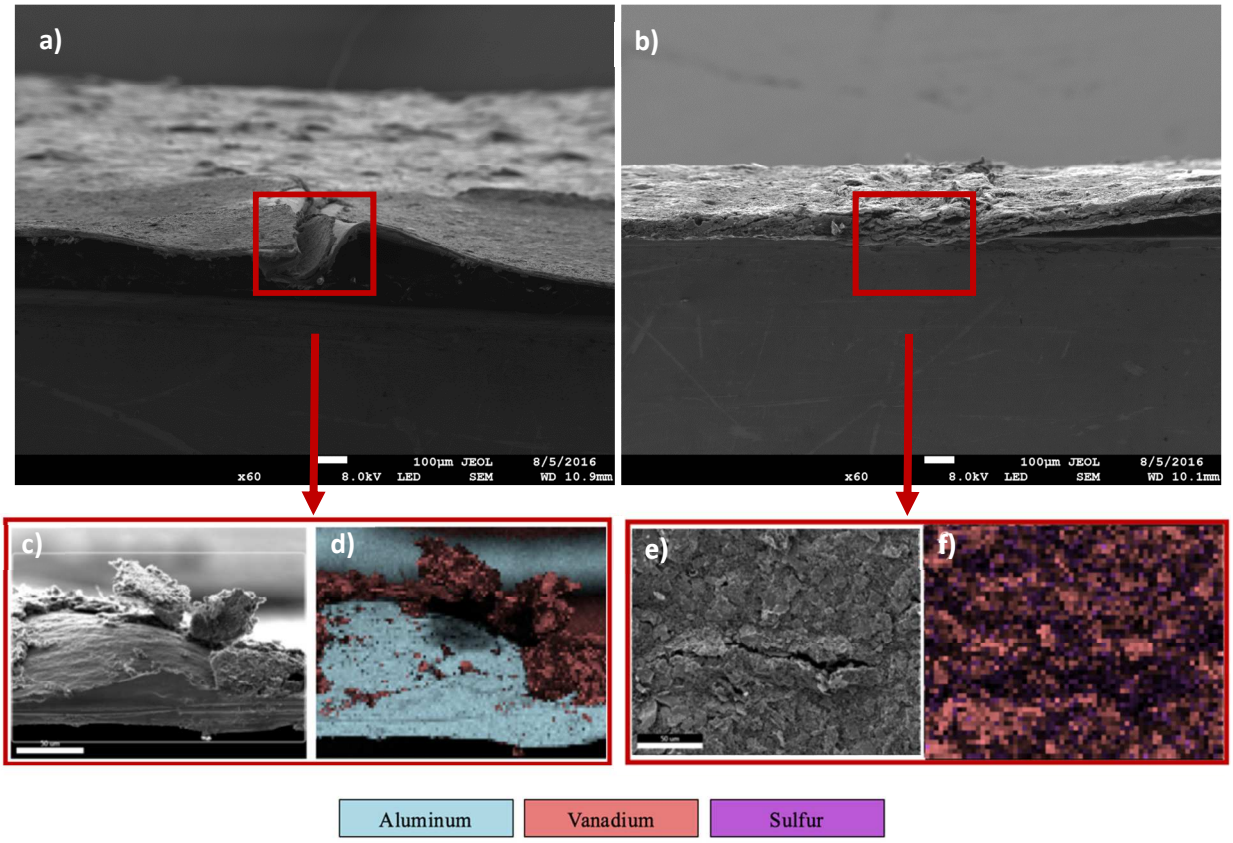

Figure 6. FESEM images of the cross-section of the a) metallic and b) paper-based electrode after bending test samples, all electrodes were bend 90º for 20 times, (the insets of the images are showing the trace of aluminum for metallic cells, sulfur for CNT-microfiber paper and Vanadium using the energy dissipative spectroscopy after the bending test), c) SEM, and d) EDS of the crack formation over the cross-section of the metallic electrodes, and e) SEM and f) EDS of the crack formation over the cross-section of the paper-based electrodes.

The structures of the electrodes were examined using FESEM. Figure 7 shows the structures of the cellulose microfiber, CNT-coated microfiber, and a CNT-coated microfiber with a layer of V_2O_5/G. Figure 7a shows a blunt cellulose microfiber without any coating. The inset of this figure (figure 7d) also reveals the surface porosity of the fibers. These fibers entangle with the conductive materials, such as the CNTs, through the LbL process and provide a highly conductive layer. As can be seen, the pores of the microfibers have been coated with the conductive CNT layer to provide a highly conductive surface, demonstrated in figure 7b, which shows a CNT-coated microfiber after coating with the conductive bilayers (CNT-coated microfiber). The formation of the multilayer conductive/polymer layers over the

wood microfibers is completely visible in the figure 7e. Figure 7c also shows a single CNT-coated microfiber with a layer of V_2O_5/G. The V_2O_5/G particles entangle with the fabrics of the CNT-microfiber paper current collector to form an integrated layer. Graphene rods also provide a highly conductive pathway between the V_2O_5 particles and the CNT layer on top of the cellulose microfibers. As shown in the figure 7f, the electrodes consist of the V_2O_5/G layers deposited over the CNT coated microfibers. Here, the V_2O_5/G composite particles are deposited over the CNT layer uniformly, thus the graphene sheets provides a conductive path between the V_2O_5 particles and the conductive CNT coated microfibers, hence, a highly conductive path between the active materials and the current collector layer has been established. The porosity of the microfibers also helps to form a mechanically stable layer of active material over the CNT-coated microfibers.

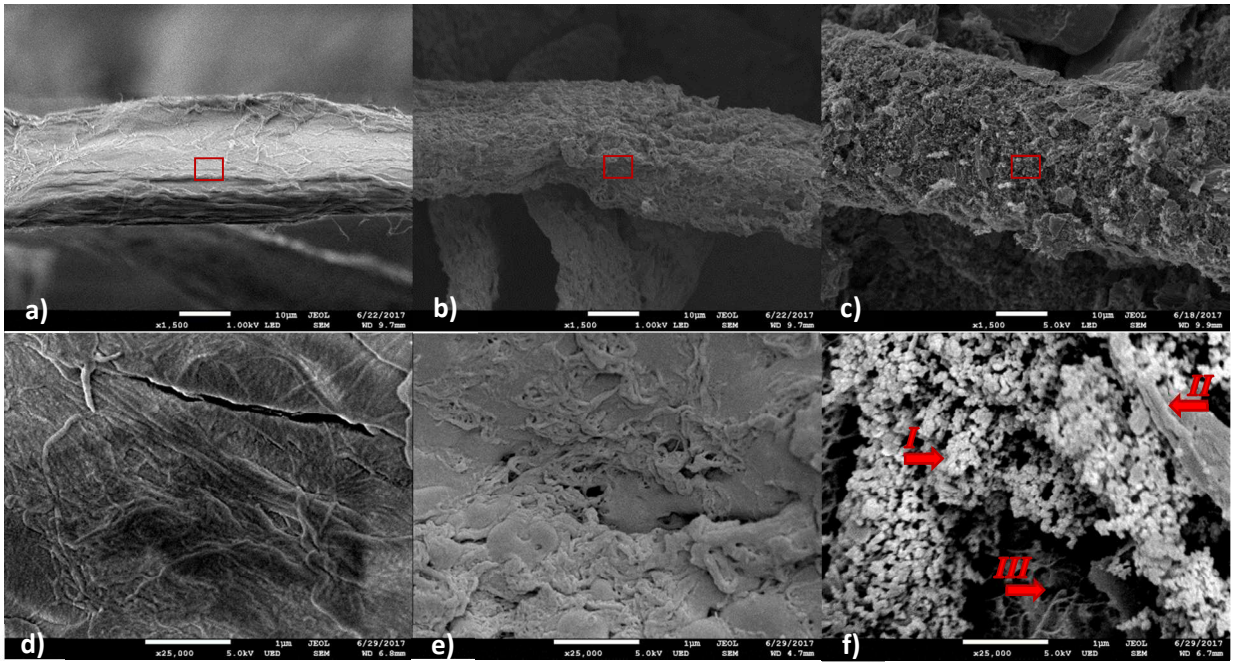

Figure 7. FESEM images: a) blunt cellulose microfiber, b) CNT-coated microfiber, and c) V_2O_5/G-coated CNT microfiber, the higher magnification images form the surface of the fibers (the red box in the top row images) of d) blunt, e) CNT-coated and f) V_2O_5/G-coated microfiber, the arrow I showing the V_2O_5/G composite particles, arrow II indicating a paper microfiber and arrow III pointing the CNT layer.

Electrochemical Stability and Impedance

The electrochemical stability of the CNT-paper and the Al foil current collectors in the electrolyte was investigated first by cyclic voltammetry, as shown in figure 8. The potential range has been limited from 1.5 to 4.0 V (*vs*. Li/Li^+) to demonstrate the typical potential range of V_2O_5 cathode materials [21]. As shown in figure 7a, no obvious redox peaks were observed for the CNT-microfiber paper in the potential range 1.5–4.0 V (*vs*. Li/Li^+), only a shuttle-shaped curve was observed, which may arise from the double layer capacitance. The Al foil was also stable in the potential range, but seemed to be starting to show some

increasing current when the potential reached 1.5 V (*vs*. Li/Li$^+$), which may correspond to the alloying of the Al and Li (figure 8a). We can conclude that the CNT-paper current collector showed better electrochemical stability compared with the conventional Al foil current collector. In some harsh conditions, such as over-discharge of a LIB cell, the potential of electrode might be forced to go below 1.00 V (*vs*. Li/Li$^+$) or approaching 0.00 V (*vs*. Li/Li$^+$) which can cause the Al corrosion [23-24]. In order to characterize the electrochemical stability of CNT-paper under over-discharge condition, a CV scan from 0.0 to 4.0 V (*vs*. Li/Li$^+$) was carried out for both Al foil and CNT paper. It is known that a Li-Al alloying process would happen in a low voltage close to 0.00 V (*vs*. Li/Li$^+$) [25-26], our CV scan result in potential range of 0 ~ 4.0 V (*vs*. Li/Li$^+$) showed obvious redox peaks in around 0.5 V and 2.5 V (*vs*. Li/Li$^+$) (as appointed by arrows in figure 8b). While for the CNT paper (figure 8b), there was no redox peaks observed during the wide potential range, suggesting that the CNT paper has much higher electrochemical stability for cathode under extreme conditions. Moreover, CNT paper can be used as the current collector for the anode as well because the typical potential range for anode is typically 0~2.5 V (*vs*. Li/Li$^+$), which just falls in the electrochemical stability range of the CNT paper (0~4.0 V *vs*. Li/Li$^+$).

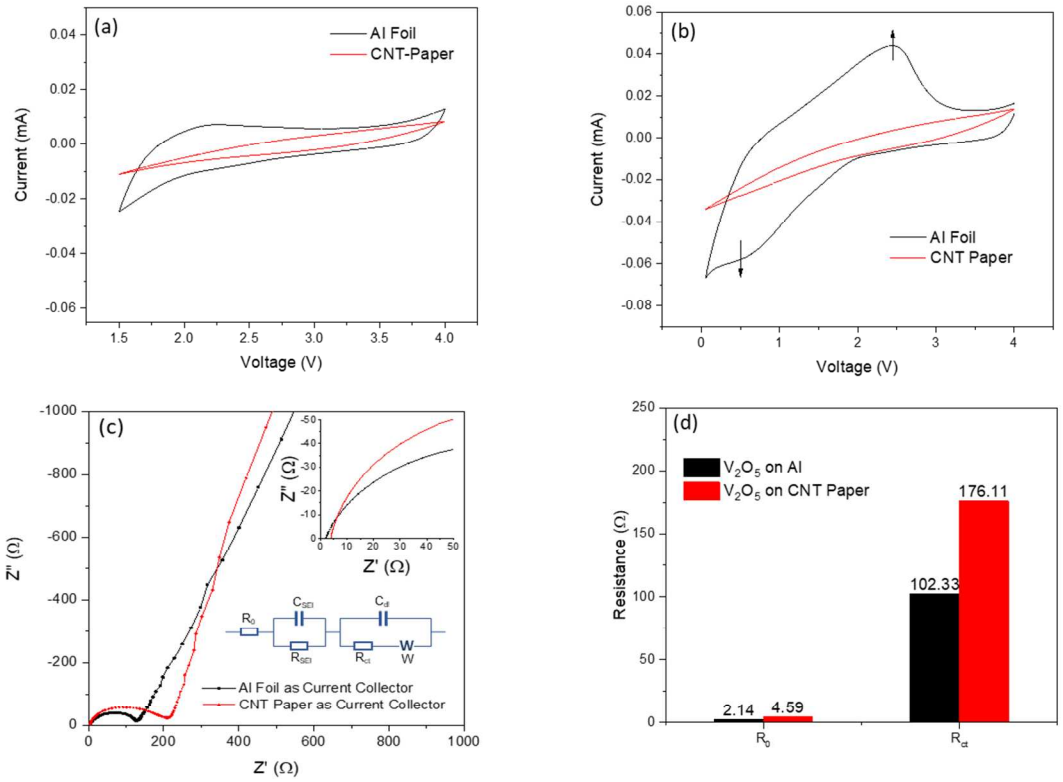

Figure 8. Electrochemical stabilities of CNT paper compared with aluminum foil at a scan range of a) 1.5 ~ 4.0 V and b) 0 ~ 4.0 V, c) impedance comparison of V_2O_5 electrodes on CNT paper and aluminum foil, and d) resistance comparison (Ohmic resistivity) of V_2O_5 electrodes on both CNT paper and aluminum foil.

Electrochemical impedance spectroscopy was also employed to characterize the resistance of the V_2O_5/G

electrode on CNT paper and Al foil. As shown in figure 8c, the CNT has relatively higher (but comparable) resistance than Al foil. An equivalent circuit model, as shown in figure 8c (inset), was used to fit the curves. R_0, which includes the ohmic resistance from the electrodes, the electrolyte, the current collectors, the separator, and the connections between them typically can be obtained from the interception of the high frequency loop and the *x* axis; R_{SEI} and C_{SEI} refer to the resistance and capacitance of the SEI layer, separately, for which the high frequency loop stands. R_{ct} and C_{dl} stand for the charge-transfer resistance and the double-layer capacitance in the electrode, respectively, which correspond to the medium frequency arc; σ refers to the Warburg diffusion impedance, which could reflect the diffusion of the Li-ion in the electrode in correspondence to the 45º line following the second arc. The impedance results shown in figure 8d were fitted with this equivalent circuit[27-28]. The V_2O_5/G electrodes on CNT paper showed relatively higher Ohmic resistance and charge transfer resistance, which might be due to the extremely low loading of the CNT fibers.

Cell Performances

In our previous work [21], with the introduction of a small amount of graphene into the V_2O_5, the reversible charge/discharge capacity of 438mAh/g was achieved, which nearly reaches the theoretical specific capacity (443 mAh/g) and shows a greatly enhanced cycle life. The capacity is much higher than current commercially available cathode materials, such as $LiFePO_4$ (165 mAh/g) [29], $LiCoO_2$ (148 mAh/g) [30], $LiNi_{0.33}Mn_{0.33}Co_{0.33}O_2$ (160 mAh/g) [31], and $LiMn_2O_4$ (120 mAh/g) [11]. Figure 9a shows the voltage profiles of the initial galvanostatic charge/discharge cycles of V_2O_5/G on Al and CNT paper, respectively. A specific capacity of 396 mAh/g has been achieved at 0.1 C (figure 9a) for the V_2O_5/G on CNT paper, compared with 406 mAh/g for V_2O_5/G on Al foil. While the amount of CNT over the paper fibers is negligible compared to that of V_2O_5, the CNT does not involve in charge/discharge capacity of the fabricated cells. In addition to the high specific capacity, this V_2O_5/G on CNT paper shows excellent reversibility (capacity retention at 1 C cycling), as shown in figure 9b, and is even better than the V_2O_5/G on Al foil (81.2% for CNT vs. 72.6% for Al), which indicates that the CNT paper could be a promising candidate for a current collector material for lithium-ion batteries. The Coulombic efficiency of V_2O_5/G on CNT paper is close to 100% and is comparable with V_2O_5/G on Al foil. Figure 9c shows the cell performance after 3-times of 180º bending. The initial capacity loss of the electrode on CNT paper after bending was found to be 9.8 mAh/g and was only a 3.3% capacity loss, while the capacity loss of the electrode on Al foil was 119.9 mAh/g, which lost 37.9% capacity of the pristine electrode before bending. These results agree with our FESEM observation that the capacity loss was a result of the active material detachment from the current collector. The capacity after 100 cycles of the electrode on CNT paper was 1.66 times higher than that of

the Al foil. The average Coulombic efficiency of the CNT paper electrode during 100 cycles (97.93%) was also slightly higher than that for the Al foil electrode (95.92%). It is speculated that after bending, the CNT paper holds the electrode materials better and keeps more materials electronically conductive than the Al foil. The rate performances of V_2O_5/G electrode on CNT paper and Al foil are shown in figure 9d. The electrode on CNT paper has comparable specific capacity at lower rates with that on Al foil, while at higher rates (i.e., 5 C and 10 C) the paper-based electrode has relatively higher specific capacity (5.6% higher @ 5 C, and 14.0% higher @ 10 C) than that of the electrode on Al foil. After bending, the electrode on CNT paper still retains a high capacity: 376 mAh/g at 0.1 C, 368 mAh/g at 0.2 C, 335 mAh/g at 0.5 C, 283 mAh/g at 1 C, 262 mAh/g at 2 C, 227 mAh/g at 5 C and 206 mAh/g at 10 C, while those of electrodes on Al foil keep the relative lower capacity: 296 mAh/g at 0.1 C, 257 mAh/g at 0.2 C, 235 mAh/g at 0.5 C, 196 mAh/g at 1 C, 154 mAh/g at 2 C, 112 mAh/g at 5 C and 93 mAh/g at 10 C (figure 9d). This corresponds to a 27.0, 43.2, 42.6, 44.4, 70.1, 102.7 and 121.5% specific capacity increase at the different rates, respectively. Such a huge improvement of rate performance of the electrodes on CNT paper over the electrodes on Al foil after bending test suggests that the CNT paper can keep electrode material more adhesive and more conductive than Al foil. The same trend can be clearly seen from the results of cyclic voltammetry (CV) scan, shown in figure 9e and f. With the similar CV curves for electrodes on CNT paper before bending (solid arrows shown in figure 9e) and after bending (dashed arrows shown in figure 9e), the CV curves of electrodes on Al foil changed drastically from more symmetric redox peaks (solid arrows shown in figure 9f) to shuttle-shaped curve without any obvious redox peaks. Such CV curve changes indicate that an additional charge transfer barrier appears after bending test, resulting from the worsen electric contact between current collector and active material causes. After the bending test, the apparent diffusion coefficient of V_2O_5/G electrode calculated from EIS, dropped 12.2% and 55.1% for electrodes with CNT-paper and Al foil as current collectors respectively, as shown in figure 9g. This suggests that the CNT paper can hold more active material than Al foil after bending, consequently, causing the lower drop on electric conductivity for the electrode of paper-based than that of Al foil based while the bending should not affect the true diffusion coefficients which only depend on the V_2O_5/G active material and the temperature. All the apparent diffusion coefficients were calculated by the surface area of all electrode material.

In summary, the use of CNT paper with a good mechanical property and excellent electrochemical stability can significantly improve the quality and flexibility of the electrode and take advantage of the ultra-high capacity and stability of V_2O_5/G materials.

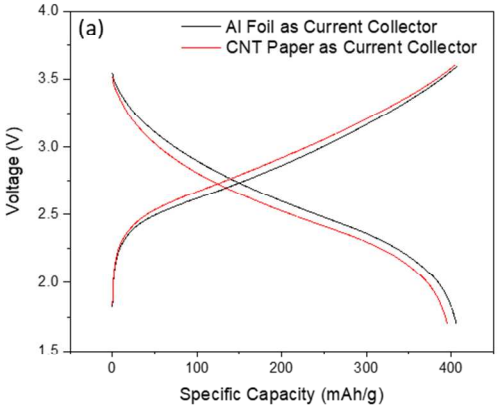
(a)
Al Foil as Current Collector
CNT Paper as Current Collector
Voltage (V)
Specific Capacity (mAh/g)

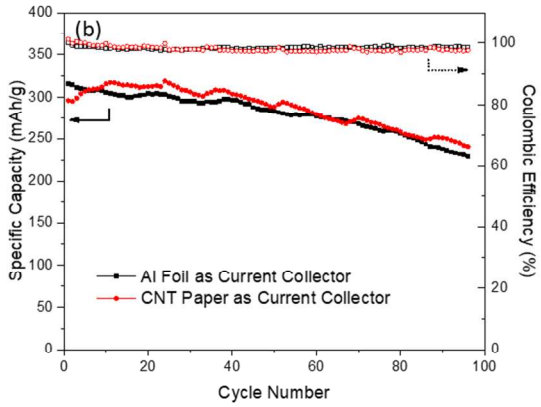
(b)
Specific Capacity (mAh/g)
Coulombic Efficiency (%)
Al Foil as Current Collector
CNT Paper as Current Collector
Cycle Number

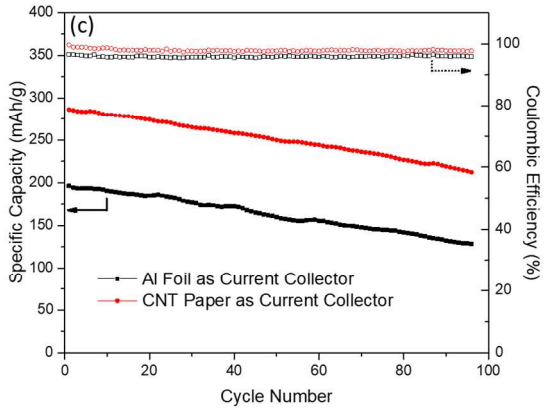
(c)
Specific Capacity (mAh/g)
Coulombic Efficiency (%)
Al Foil as Current Collector
CNT Paper as Current Collector
Cycle Number

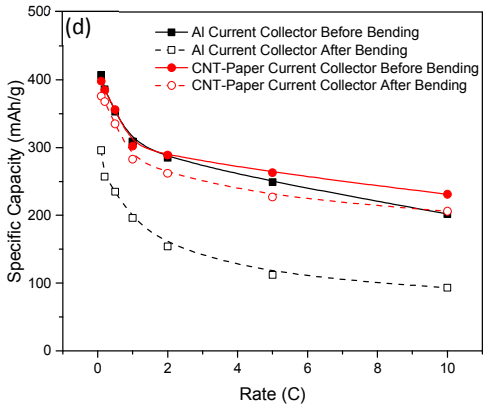
(d)
Al Current Collector Before Bending
Al Current Collector After Bending
CNT-Paper Current Collector Before Bending
CNT-Paper Current Collector After Bending
Specific Capacity (mAh/g)
Rate (C)

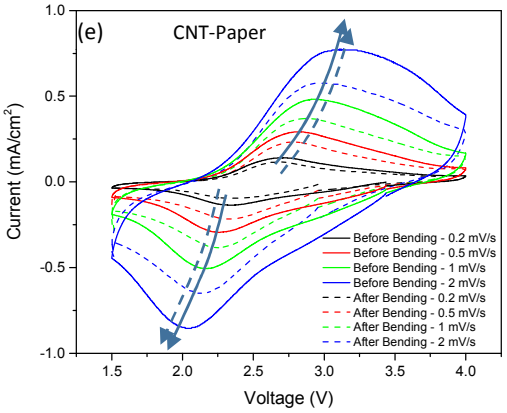
(e)
CNT-Paper
Current (mA/cm²)
Voltage (V)
Before Bending - 0.2 mV/s
Before Bending - 0.5 mV/s
Before Bending - 1 mV/s
Before Bending - 2 mV/s
After Bending - 0.2 mV/s
After Bending - 0.5 mV/s
After Bending - 1 mV/s
After Bending - 2 mV/s

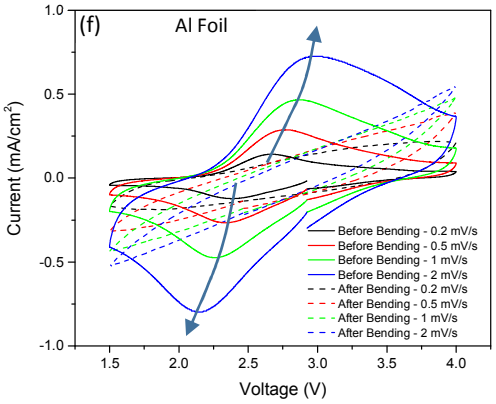
(f)
Al Foil
Current (mA/cm²)
Voltage (V)
Before Bending - 0.2 mV/s
Before Bending - 0.5 mV/s
Before Bending - 1 mV/s
Before Bending - 2 mV/s
After Bending - 0.2 mV/s
After Bending - 0.5 mV/s
After Bending - 1 mV/s
After Bending - 2 mV/s

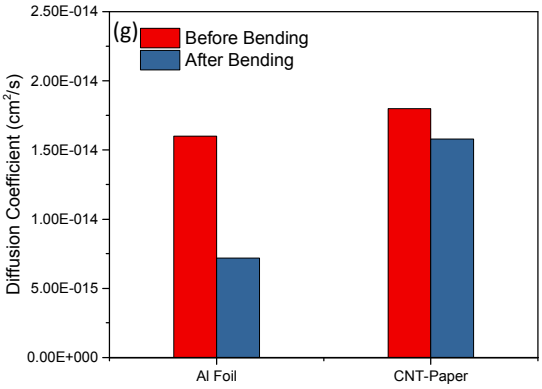

Figure 9. Electrochemical performance of the V_2O_5 electrode on CNT paper. a) Initial charge/discharge voltage profiles of the V_2O_5 electrode on both Al foil and CNT paper, C-rate: 0.1 C, cut-off voltage: 1.7~3.6 V. b) Specific capacity and Coulombic efficiency with cycle number of the V_2O_5 electrode on both Al foil and CNT paper; C-rate: 1 C, cut-off voltage: 1.7~3.6 V. c) Specific capacity and Coulombic efficiency with cycle number of the V_2O_5 electrode on both Al foil and CNT paper after 3 180º bending; C-rate: 1 C, cut-off voltage: 1.7~3.6 V. d) Rate performance before and after bending. e) CV curves at different scan rates of V_2O_5/G electrode with CNT-paper as current collector before (solid) and after (dashed) bending; scan rate: 0.1~2 mV/s, voltage range: 1.5 ~ 4 V. f) CV curves at different scan rates of V_2O_5/G electrode with Al foil as current collector before (solid) and after (dashed) bending; scan rate: 0.1~2 mV/s, voltage range: 1.5 ~ 4 V. g) Apparent diffusion coefficient of V_2O_5/G electrodes on CNT-paper and Al foil as current collectors before and after bending.

Conclusion

A CNT-microfiber paper was made by a layer-by-layer (LBL) assembly of highly conductive materials, such as carbon nanotubes over wood microfibers, into a sheet. The electrochemical stability of this conductive paper was characterized and proved that it can be used as the current collector for a cathode, providing simple fabrication, high safety, lower weight, and more flexibility to lithium-ion batteries. The nanostructured V_2O_5/Graphene hybrid composite was applied to the CNT-microfiber paper current collectors and demonstrated excellent performance, achieving around 396 mAh/g at 0.1 C and 300 mAh/g at 1 C with more than 80% capacity retention after 100 cycles. CNT-microfiber paper is a promising candidate as current collector for high-performance electrodes to construct flexible LIB cells.

Acknowledgement

The authors would like to thank the National Science Foundation Major Research Instrumentation Program for support (Award # 1229514) for the FESEM and (Award # 1429241) for XRD. Any opinions, findings, and conclusions or recommendations expressed in this material are those of the author(s) and do not necessarily reflect the views of the National Science Foundation. The authors would like to thank Ms.

Bhavya Sri Pakki for her assistance in the laboratory and Dr. Daniel Minner for his assistance with the instrumentation.

References

(1) Kwon, Y. H.; Woo, S. W.; Jung, H. R.; Yu, H. K.; Kim, K.; Oh, B. H.; Ahn, S.; Lee, S. Y.; Song, S. W.; Cho, J. Cable□Type Flexible Lithium Ion Battery Based on Hollow Multi□Helix Electrodes. *Adv. Mater.* **2012,** *24* (38), 5192-5197.

(2) Song, Z.; Ma, T.; Tang, R.; Cheng, Q.; Wang, X.; Krishnaraju, D.; Panat, R.; Chan, C. K.; Yu, H.; Jiang, H. Origami Lithium-Ion Batteries. *Nat. commun.* **2014,** *5,* 3140-3146.

(3) Cheng, Q.; Song, Z.; Ma, T.; Smith, B. B.; Tang, R.; Yu, H.; Jiang, H.; Chan, C. K. Folding Paper-Based Lithium-Ion Batteries for Higher Areal Energy Densities. *Nano lett.* **2013,** *13* (10), 4969-4974.

(4) Hu, L.; Choi, J. W.; Yang, Y.; Jeong, S.; La Mantia, F.; Cui, L.-F.; Cui, Y. Highly Conductive Paper for Energy-Storage Devices. *Proc. Natl. Acad. Sci.* **2009,** *106* (51), 21490-21494.

(5) Landi, B. J.; Ganter, M. J.; Cress, C. D.; DiLeo, R. A.; Raffaelle, R. P. Carbon Nanotubes for Lithium Ion Batteries. *Energy Environ. Sci.* **2009,** *2* (6), 638-654.

(6) Aliahmad, N.; Agarwal, M.; Shrestha, S.; Varahramyan, K. Based Lithium-Ion Batteries Using Carbon Nanotube-Coated Wood Microfibers. *IEEE Trans. Nanotechnol.* **2013,** *12* (3), 408-412.

(7) Aliahmad, N.; Shrestha, S.; Varahramyan, K.; Agarwal, M. Poly (Vinylidene Fluoride-Hexafluoropropylene) Polymer Electrolyte for Paper-Based and Flexible Battery Applications. *AIP Adv.* **2016,** *6* (6), 065206.

(8) Agarwal, M.; Lvov, Y.; Varahramyan, K. Conductive Wood Microfibres for Smart Paper through Layer-by-Layer Nanocoating. *Nanotechnology* **2006,** *17* (21), 5319.

(9) Lin, F.; Markus, I. M.; Nordlund, D.; Weng, T. C.; Asta, M. D.; Xin, H. L.; Doeff, M. M. Surface Reconstruction and Chemical Evolution of Stoichiometric Layered Cathode Materials for Lithium-Ion Batteries. **2014,** *5*, 3529, DOI: 10.1038/ncomms4529

(10) Huang, H.; Yin, S. C.; Nazar, L. s. Approaching Theoretical Capacity of Lifepo4 at Room Temperature at High Rates. *Electrochem. Solid-State Lett* .**2001,** *4* (10), A170-A172.

(11) Lee, M. J.; Lee, S.; Oh, P.; Kim, Y.; Cho, J. High Performance $LiMn_2O_4$ Cathode Materials Grown with Epitaxial Layered Nanostructure for Li-Ion Batteries. *Nano Lett.* **2014,** *14* (2), 993-999, DOI: 10.1021/nl404430e.

(12) Park, J. W. *Effects of Non-Uniform Temperature on in-Situ Current Distribution and Non-Uniform State of Charge Measurements for Lifepo 4 and Linimncoo 2 Cells*, 231st ECS Meeting (May 28-June 1, 2017), Ecs: 2017.

(13) Guan, D.; Jeevarajan, J. A.; Wang, Y. Enhanced Cycleability of Limn2o4 Cathodes by Atomic Layer Deposition of Nanosized-Thin Al_2O_3 Coatings. *Nanoscale* **2011,** *3* (4), 1465-1469.

(14) Cao, A. M.; Hu, J. S.; Liang, H. P.; Wan, L. J. Self□Assembled Vanadium Pentoxide (V2o5) Hollow Microspheres from Nanorods and Their Application in Lithium□Ion Batteries. *Angew. Chem., Int. Ed.* **2005,** *44* (28), 4391-4395.

(15) Mai, L.; Xu, L.; Han, C.; Xu, X.; Luo, Y.; Zhao, S.; Zhao, Y. Electrospun Ultralong Hierarchical Vanadium Oxide Nanowires with High Performance for Lithium Ion Batteries. *Nano Lett.* **2010,** *10* (11), 4750-4755.

(16) Pan, A.; Zhang, J. G.; Nie, Z.; Cao, G.; Arey, B. W.; Li, G.; Liang, S.-q.; Liu, J. Facile Synthesized Nanorod Structured Vanadium Pentoxide for High-Rate Lithium Batteries. *J. Mater. Chem.* **2010,** *20* (41), 9193-9199.

(17) Mai, Y. J.; Wang, X. L.; Xiang, J. Y.; Qiao, Y. Q.; Zhang, D.; Gu, C. D.; Tu, J. P. Cuo/Graphene Composite as Anode Materials for Lithium-Ion Batteries. *Electrochim. Acta* **2011,** *56* (5), 2306-2311.

(18) Wang, Y.; Takahashi, K.; Lee, K. H.; Cao, G. Nanostructured Vanadium Oxide Electrodes for Enhanced Lithium□Ion Intercalation. *Adv. Funct. Mater.* **2006,** *16* (9), 1133-1144.

(19) Gu, L.; Zhu, C.; Li, H.; Yu, Y.; Li, C.; Tsukimoto, S.; Maier, J.; Ikuhara, Y. Direct Observation of Lithium Staging in Partially Delithiated Lifepo4 at Atomic Resolution. *J. Am. Chem. Soc.* **2011,** *133* (13), 4661-4663, DOI: 10.1021/ja109412x.

(20) Li, Z. F.; Zhang, H.; Liu, Q.; Liu, Y.; Stanciu, L.; Xie, J. Hierarchical Nanocomposites of Vanadium Oxide Thin Film Anchored on Graphene as High-Performance Cathodes in Li-Ion Batteries. *ACS Appl. Mater. Interfaces* **2014,** *6* (21), 18894-18900, DOI: 10.1021/am5047262.

(21) Liu, Q.; Li, Z. F.; Liu, Y.; Zhang, H.; Ren, Y.; Sun, C. J.; Lu, W.; Zhou, Y.; Stanciu, L.; Stach, E. A. Graphene-Modified Nanostructured Vanadium Pentoxide Hybrids with Extraordinary Electrochemical Performance for Li-Ion Batteries. *Nat. commun.* **2015,** *6,* 6127–6137.

(22) Shiraishi, S.; Kurihara, H.; Okabe, K.; Hulicova, D.; Oya, A. Electric Double Layer Capacitance of Highly Pure Single-Walled Carbon Nanotubes (Hipco™ Buckytubes™) in Propylene Carbonate Electrolytes. *Electrochem. Commun.* **2002,** *4* (7), 593-598.

(23) He, H.; Liu, Y.; Liu, Q.; Li, Z.; Xu, F.; Dun, C.; Ren, Y.; Wang, M.-x.; Xie, J. Failure Investigation of Lifepo4 Cells in over-Discharge Conditions. *J. Electrochem. Soc.* **2013,** *160* (6), A793-A804, DOI: 10.1149/2.039306jes.

(24) Xu, F.; He, H.; Liu, Y.; Dun, C.; Ren, Y.; Liu, Q.; Wang, M.-x.; Xie, J. Failure Investigation of Lifepo4 Cells under Overcharge Conditions. *J. Electrochem. Soc.* **2012,** *159* (5), A678-A687, DOI: 10.1149/2.024206jes.

(25) Zhang, S.; Jow, T. Aluminum Corrosion in Electrolyte of Li-Ion Battery. *J. of Power Sources* **2002,** *109* (2), 458-464.

(26) Myung, S. T.; Hitoshi, Y.; Sun, Y.-K. Electrochemical Behavior and Passivation of Current Collectors in Lithium-Ion Batteries. *J. Mater. Chem.* **2011,** *21* (27), 9891-9911.

(27) Liu, Y.; Liu, Q.; Li, Z.; Ren, Y.; Xie, J.; He, H.; Xu, F. Failure Study of Commercial Lifepo4 Cells in over-Discharge Conditions Using Electrochemical Impedance Spectroscopy. *J. Electrochem. Soc.* **2014,** *161* (4), A620-A632.

(28) Liu, Y.; Xie, J. Failure Study of Commercial Lifepo4 Cells in Overcharge Conditions Using Electrochemical Impedance Spectroscopy. *J. Electrochem. Soc.* **2015,** *162* (10), A2208-A2217.

(29) Yamada, A.; Chung, S. C.; Hinokuma , K. Optimized Lifepo4 for Lithium Battery Cathodes. *J. Electrochem. Soc.* **2001,** *148* (3), A224-A229, DOI: 10.1149/1.1348257.

(30) Cho, J.; Kim, Y.-W.; Kim, B.; Lee, J. G.; Park, B. A Breakthrough in the Safety of Lithium Secondary Batteries by Coating the Cathode Material with Alpo4 Nanoparticles. *Angew. Chem. Int. Ed.* **2003,** *42* (14), 1618-1621, DOI: 10.1002/anie.200250452.

(31) Lin, F.; Markus, I. M.; Nordlund, D.; Weng, T. C.; Asta, M. D.; Xin, H. L.; Doeff, M. M. Surface Reconstruction and Chemical Evolution of Stoichiometric Layered Cathode Materials for Lithium-Ion Batteries. *Nat. Commun.* **2014,** *5*, 3529, DOI: 10.1038/ncomms4529

TOC:

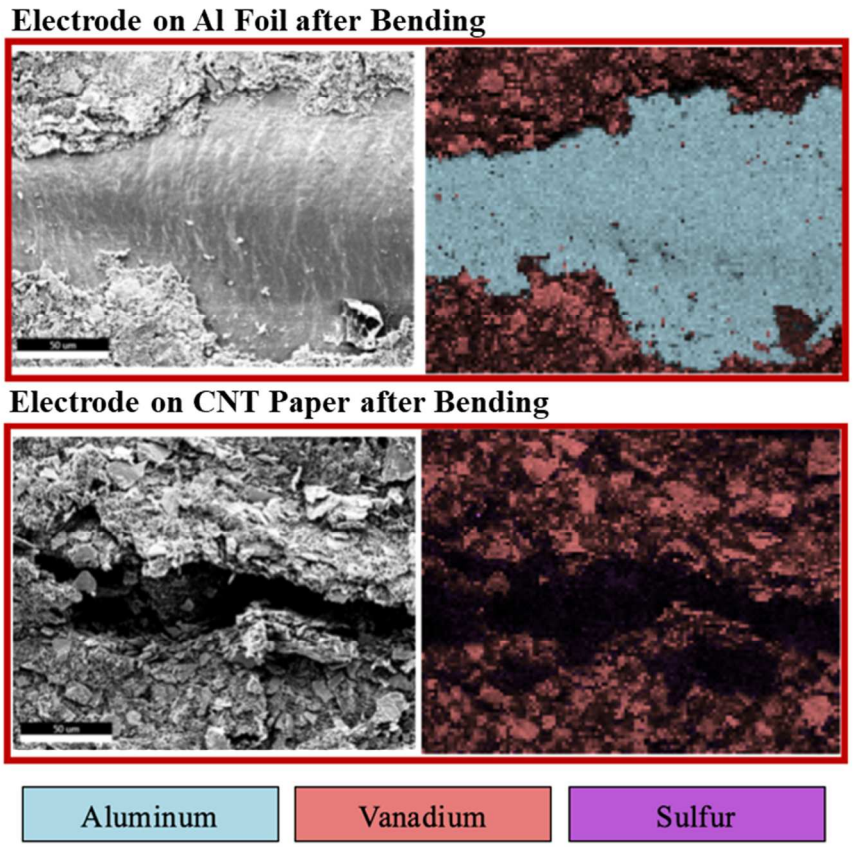
Electrode on Al Foil after Bending
Electrode on CNT Paper after Bending
Aluminum
Vanadium
Sulfur